In-situ production of Histamine-imprinted polymeric materials for electrochemical monitoring of fish

Verónica M. Serrano[1,2], Ana R. Cardoso[1,2], Mário Diniz[3], M. Goreti F. Sales[1,2]*

[1)]*BioMark/ISEP, School of Engineering of the Polytechnic Institute of Porto, Porto, Portugal*

[2)]*CEB, Centre of Biological Engineering, Minho University, Braga, Portugal*

[3)]*UCIBIO-REQUIMTE, Faculty of Science and Technology, Nova University, Lisbon, Portugal*

* To whom correspondence should be addressed: Goreti Sales, School of Engineering of the Polytechnique School of Porto, R. Dr. António Bernardino de Almeida, 431, 4200-072 Porto, Portugal. Tel: +351228340544; Fax: +351228321159. goreti.sales@gmail.com; mgf@isep.ipp.pt.

Abstract

A new electrochemical sensor for histamine (HIS) detection in fish is presented herein, prepared by tailoring a molecularly-imprinted polymer (MIP) sensing material on a gold screen-printed electrode (Au-SPEs), in which the polymeric film was generated *in-situ*. This film was obtained by electropolymerizing aniline under conditions that preserved the chemical structure of HIS. Raman spectroscopy followed the chemical changes occurring at each stage of the electrode modification.

The device performance was assessed by evaluating the changes in electron transfer properties of a standard redox probe $[Fe(CN)_6]^{4-}/[Fe(CN)_6]^{3-}$, by cyclic voltammetry (CV) and electrochemical impedance spectroscopy (EIS). EIS was also used to calibrate the sensor, having standard solutions prepared under different background media (electrolyte or a blank sample of fish extract). The device displayed a linear response from 500 nM to 1 mM, with a limit of detection of 207 nM, and a selective behaviour against tyramine, another amine related to fish degradation.

In general, the results obtained with fish samples showed that the modifications made on the sensing element were successful and that the resulting sensor detected as low as 100 nM of HIS. The final sensor provided reproducible and accurate readings of fish samples subject to degradation and was completely assembled *in-situ*, in a very simple and straightforward approach.

Keywords: Molecularly imprinted polymer; electropolymerization; screen-printed electrode; aniline; Histamine.

1. Introduction

Histamine (HIS) is a relevant biogenic amine which acts as a mediator in local hypersensitivity (called HIS intolerance or HIS poisoning). It is present in several foods, such as vegetables, fruit, fermented foods, and specially in fish [1], [2], with established legal limits for human consumption and mostly found in fishery products. If its concentration is lower than 10 mg/kg, it indicates that the fish is of good quality. Amounts higher than 30 mg/kg means significant deterioration, and a level of 50 mg/kg or higher is an evidence of decomposition [2], [3]. Furthermore, scombroid poisoning from HIS is associated with some specific fish species such as tuna, mackerel, sardine, herring, and anchovy [4]. All these suggest the development of low-cost and quick methods for His determination *in-situ*.

Conventional methods employed to determine HIS are essentially chromatographic-based, thereby being restricted to laboratorial facilities and sometimes requiring sample derivatization, being therefore unsuitable for routine and on-site analysis of HIS [5]. Alternative methods include HIS biosensors, combining a biorecognition element with a suitable transduction scheme. In general, electrochemical-based biosensors offer high sensitivity and selectivity, simplicity, precision, rapid response and low cost of instrumentation [4]–[6].

There are many electrochemical biosensors developed to target HIS. In general, their main difference is related to the nature of the biorecognition element, from which enzymes or antibodies are highlighted. Table 1 lists several enzyme-based biosensors found in the literature, employing different enzymes, in different combinations and different electrode supports, established by a direct product detection or involving a secondary enzyme reaction. Table 2 lists the few antibody-based HIS biosensors found in the literature. In these, HIS detection is performed directly or in a competition assay, involving in some works redox mediators. Overall, enzymes and antibodies are naturally derived materials that display excellent selectivity features but also have high cost and little stability under different conditions (humidity, temperature, pH and ionic content).

As an alternative to naturally-derived biorecognition elements, there are biomimetic materials such as molecularly-imprinted materials (MIPs) that may also offer high selectivity, rapid detection, and *in-situ* application feasibility [7]. In general, MIPs are synthetic materials prepared by polymerizing functional and cross-linking monomers around the target template, which afterwards is extracted to generate binding sites with complementary shape, size and functionalities [8]. Also, MIPs offer easy preparation, good stability, low cost, and robustness [9], [10].

Moreover, the selection of an electrical stimulus to initiate the polymerization is also an expeditous approach to produce MIP materials *in-situ*. Electrochemical techniques allow a strict control of the electrical parameters to be established at the electrode surface, thereby ensuring a strict control of the polymer growth. These are essential features to ensure the production of highly reproducible materials and consequently highly reproducible sensing devices. Yet, this is not easy when the target molecule itself undergoes oxidation under low potential values [11], which is the case of HIS. This needs the careful selection of electrical and chemical conditions that allow a differential oxidation process between monomer and target molecule. This explains why there are few MIP materials for HIS [12] and, as far as we know, why there is only a single work producing the MIP by electropolymerization [13]. The later is a piezoelectric (acoustic) sensor that employs two distinct bis(bithiophene) derivatives as monomers, and that cannot be compared with electrochemical biosensors, especially in terms of cost and feasibility to perform analysis on-site.

Thus, as far as we know, this work presents for the first time an HIS electrochemical biosensor prepared by *in-situ*, by assembling a MIP material with electropolymerized aniline. Aniline is used to make dyes and drugs, during the redox reaction and its polymerization yields polyaniline (PANI) [14]. PANI is a unique polymer, which has good electrical properties, good stability and reasonable cost [15]. The MIP film was therefore obtained by selecting the optimal conditions to establish a polyaniline-based imprinted film. The resulting biosensor was characterized and applied to determine HIS in fish samples (sardine and mackerel).

2. Experimental Section

2.1. Apparatus

The electrochemical measurements were obtained by using a potentiostat/galvanostat/impedance analyzer from PalmSens4, controlled by PSTrace electrochemistry software. The Gold Screen-Printed Electrodes (Au-SPEs) were purchased from DropSens (DRP-220AT) and contained a silver reference electrode, a gold auxiliary electrode and a gold working electrode (4 mm diameter). Au-SPEs were linked to the potentiostat via a switch box produced by BioTID Electrónica.

2.2. Reagents

Along this work, ultrapure Milli-Q water laboratory grade (conductivity <0.1 µS/cm) was used. Potassium hexacyanoferrate II-3-hydrate ($K_4[Fe(CN)_6]\cdot 3H_2O$) and potassium hexacyanoferrate III ($K_3[Fe(CN)_6]$) were obtained from Riedel-deHäen; cysteamine chlorohidrate ($HSCH_2CH_2NH_2\cdot HCl$) were purchased from Merck; HIS dihydrochloride, ≥99%, lithium perchlorate and sulfuric acid 95-97% (H_2SO_4) were obtained from Sigma-Aldrich; aniline (C_6H_7N) was obtained from Analar Normapur; phosphate buffered saline (PBS) tablets from Amresco; tyramine (TYR) from Sigma Aldrich.

2.3. Solutions

All solutions were prepared in ultrapure water. A 0.50 M H_2SO_4 solution was used to clean the commercial SPEs. A 0.05 M cysteamine solution was prepared in ultrapure water. The MIP film was assembled with a solution of 0.01 M HIS and 0.01 M aniline, prepared in 0.20 M lithium perchlorate (polymerization mixture). A non-imprinted polymer (NIP) material was prepared as control, using only 0.01 M aniline in 0.20 M of lithium perchlorate. The selectivity study compared the competitive behavior of a 10 µM HIS solution, and a mixture of HIS and TYR with the same concentration (10

µM), both prepared in 0.20 M lithium perchlorate. HIS standard solutions used in the calibrations were also prepared in 0.20 M lithium perchlorate and ranged 1.0×10^{-7} to 1.0×10^{-2} M. The electrical changes occurring at the surface were followed by a solution of 5 mM $[Fe(CN)_6]^{4-}$ and $[Fe(CN)_6]^{3-}$, prepared in 0.1 M PBS.

2.4. Preparation of electrochemical biosensor on Au-SPE

The working Au-SPE surface was cleaned by electrochemical treatment, using CV from –0.1 at 1.5 V, with scan rate of 0.05 V, for 5 cycles, in 0.50 M H_2SO_4. Afterwards, the gold surface was washed with ultrapure water. The next step consisted in the incubation of 0.05 M Cysteamine, for 1h. The MIP layer was produced by chrono-amperometry, at +0.55V for 150s, using the polymerization mixture. Finally, the template was removed by incubating the film in ultrapure water, for 15 minutes.

2.5. Raman Analysis

Raman spectroscopy analysis was used to follow each step of the MIP/NIP assembly. This was done by direct analysis of the material in a Thermo Scientific DXR Raman Spectroscope, equipped with a 785 nm laser. The average signal-to-noise ratio (peak height/RMS noise) was allowed for 900 seconds, after 10 minutes photo bleaching, using a 1 mW laser power and a 50 µm pinhole aperture.

2.6. Electrochemical Procedures

All electrochemical assays were repeated three times. CV assays scanned potentials from -0.5 to +0.5 V, at 0.05 V/s, yielding information about redox potential and electrochemical reaction rates. EIS assays were performed at an open circuit potential, using a sinusoidal wave with an amplitude of 0.01 V, and 50 data points, logarithmically distributed over 0.1 – 100000.0 Hz frequency range. The EIS data fitted a Randles equivalent circuit, using 5.5 PSTrace from PalmSens, and was analyzed by

142 Nyquist plots, reflecting the mixed kinetic process taking place at the electrode-electrolyte interface
143 that could be expressed as the real part of the impedance (Z'), which is the resistance, and its imaginary
144 part (Z''). The charge- transfer resistance (R_{ct}) was measured by the diameter of the semi-circle in the
145 Nyquist plot. Square wave voltammetry (SWV) was also used, providing a sensitive and selective
146 technique [16], and scanning potentials from –0.2 to +0.8 V.

147 The changes in the electrical properties of the sensing surface monitored the response of the redox
148 probe solution. The limit of detection (LOD) was the concentration corresponding to $x+3\sigma$, as extracted
149 from the linear response, where x was the average value of the blank signals and σ the corresponding
150 standard deviation [17]. For the selectivity studies, a competitive assay between HIS and a different
151 biogenic amine usually found in fishery products was performed, using both molecules in the same
152 concentration. In these studies, two independent devices were necessary to test the single HIS solution
153 and the mixed solution of HIS and biogenic amine (10 µM). The interfering specie selected for this
154 assay was TYR [2].

155

156 3.8 Histamine analysis by ELISA:

157 Fish samples were also assessed for the content of histamine (HIS) using an indirect Enzyme Linked
158 Immunosorbent assay (ELISA). In brief, samples were coated (50 µL/well) on 96-well microplates
159 (Greiner Microlon, Germany) and allowed to incubate overnight at 4°C. Then, the microplate was
160 washed (3X) in a washing solution (phosphate buffer solution with 0.05 Tween-20) and then blocked
161 by adding 200 µL of 1% BSA (Bovine Serum Albumin, Nzytech, Portugal). After 2h incubation the
162 blocking solution was discharged, and the microplate washed (3X) once again with the washing
163 solution. Afterwards, a HIS monoclonal antibody (anti-Histamine (HIS) antibody, antibodies-online
164 GmbH, germany) was diluted to an appropriate concentration (1:200) and added to each well. The
165 microplate was incubated at 37 °C for 90 min. After another washing step, the secondary antibody

(anti-mouse IgC, fc specific, conjugated for alkaline phosphatase, Sigma-Aldrich, Germany) was diluted (1:1000 in 1% BSA) and 50 µl added to each well followed by another incubation stage (37 °C for 90 min). After washing, 50µl of p-nitrophenyl phosphate substrate solution (PNPP tablets, Sigma-Aldrich) was added to each well and incubated for 30 min at room temperature. Then, 100µl of 3M NaOH stop solution was added to each microplate well and the absorbance was read using a microplate reader at 405 nm (Biotek Synergy HTX, USA). For quantification, HIS standards were prepared by serial dilutions of purified carp HIS (Histamine analytical standard, Sigma-Aldrich, germany) to give a range from 20 to 2000 ng/mL.

3. Results and Discussion

3.1. Electrode pre-treatment

The practical use of SPEs requires their previous cleaning, in order to ensure reproducible electrochemical features among different units. To this end, three different treatments for cleaning the gold surface were tested: (i) cleaning the surface with absolute ethanol (2×); (ii) cleaning with absolute ethanol (2×) followed by electrochemical CV cleaning with H_2SO_4; (iii) or using only an electrochemical stage, by CV, using a sulfuric acid solution. The potential applied in electrochemical cleaning and its duration were also optimized in previous assays, suggesting the favorable use of –0.1 to 1.5 V, along 5 CV cycles. The condition selected for further electrode cleaning was electrochemical cleaning, considering the resulting R_{ct} decrease in the Nyquist plot and the increasing electrode reproducibility among different SPE units. Typical CV and EIS plots obtained under this condition are shown in

Figure 1A.

Before the MIP assembly, the clean gold electrode was modified to generate an amine layer. This amine layer would participate in the electropolymerization of aniline through its amine groups, thereby ensuring that the MIP film would be stably linked to the electrode layer. Cysteamine was used for this purpose, binding to the gold layer through its thiol group, -SH, and leaving the amine groups exposed to the outer surface [18]. As expected, the addition of cysteamine contributed to an R_{ct} increase, although of small significance when compared to the clean electrode (Figure 1A). The resulting surface is identified by Au/Cys.

3.2. Selecting the electrochemical conditions for polymerization

The production of the MIP layer by electropolymerization requires the formation of radical species from the monomer compounds, by applying specific electrical conditions at the electrode surface. To ensure that the polymerization taking place at the electrode was not involving HIS, it was necessary to ensure that the selected electrical conditions would not affect the structure of HIS. If this would happen, HIS would co-polymerize with aniline and stay permanently bounded to the polymeric layer, thereby limiting the formation of binding sites.

For this purpose, the electrochemical features of aniline and HIS were first studied in single solutions and after in mixed solutions. The first tests allowed confirming that HIS and aniline were both electroactive in aqueous solutions in similar potential ranges. Thus, other background media were tested trying to identify a condition in which HIS would be inactive under an applied potential and aniline would remain electroactive under the same potential range. To this end, HIS solutions were prepared in 0.20 M ACN, 0.20 M lithium perchlorate and 0.20 M DMSO and electrochemically tested. The results obtained are shown in Figure S1. In general, it was found that HIS was no longer electroactive within –1.0 to +1.0V when lithium perchlorate was used as dissolution medium (verified

212 for concentrations up to 0.01 M HIS). In contrast, the electroactivity of aniline persisted under these
213 conditions, thereby ensuring the possibility of forming PANI without altering the structure of HIS.

214

215 ### *3.3. Assembly of the sensing layer*

216 The MIP film was obtained by bulk electropolymerization, in which specific electrical conditions were
217 applied to a solution containing both monomer (aniline) and template (HIS). This was done by bulk
218 polymerization, which is the most common imprinting approach for producing MIP materials for small
219 size target molecules. In this, a pre-polymer arrangement is allowed to be formed between HIS and
220 aniline, which is expected to involve hydrogen bond interactions. After this, the polymeric network is
221 formed by a radical reaction, initiated by giving enough potential to generate oxidized radicals of
222 aniline. In agreement with the data in Figure S2, a chrono-amperometric procedure involving the
223 application of a potential of +0.55 V, for 150s, was established. The MIP electrode (Au/Cys/MIP) was
224 obtained by electropolymerizing a mixed solution of aniline and HIS, while the NIP electrode
225 (Au/Cys/NIP, the control) was produced by using a solution of only Aniline.

226 The resulting CV and EIS data is shown in Figure 1B. Overall, the presence of the resulting polymeric
227 layer was confirmed by the peak current decrease of the standard redox probe in the cyclic
228 voltammogram (Figure 1 B1) and the R_{ct} increase in the Nyquist plot (Figure 1 B2), when compared
229 to the Au/Cys surface.

230 Moreover, there was a significant different between MIP and NIP electrodes, which reflected the effect
231 of the presence of HIS in the MIP material, because this was the single experimental difference in both
232 materials. The CV assays of the Au/Cys/MIP electrode showed much lower peak currents and a higher
233 separation of peaks (Figure 1 B1), than the Au/Cys/NIP electrode. Consistently, the R_{ct} value was
234 much higher in the MIP film, thereby confirming the presence of HIS within the polymeric network.
235 (Figure 1 B1). Overall, the presence of HIS on the growing polymer changed the electrical properties
236 of the surface at the moment of polymer film growth. This could reflect the non-conductive properties

of HIS itself and/or the change of the electrical features of the PANI film formed therein, especially because the conductive features of the PANI films is intrinsically linked to the conditions established for its polymerization [19]. In addition, the formation of less conductive polymeric layers in the first stages of the MIP polymerization contributed to the formation of less radicals per unit time at the external surface, and the rate of polymer formation decreased as the polymer was growing.

The reproducibility of independent electrodes was further tested and presented in Figure 2. Overall, the CV and ESI data confirmed the good reproducibility of the electrochemical events, considering that three independent electrodes of Au/Cys/MIP (Figure 2A) and Au/Cys/NIP (Figure 2B) were involved herein and that each Au-SPE is intrinsically different as purchased.

3.4. Removal of HIS from the sensing layer

The final step of the MIP assembly was to remove the HIS template from the polymeric network. By removing HIS, binding sites of complementary shape to the target molecule would be formed within the polymeric network [20], [21]. Since HIS is highly soluble in water, this would be a good solvent to remove the molecule from the imprinted surface, thereby avoiding the use of other reagents that could alter intrinsic characteristics or damage the PANI layer.

The efficiency of the HIS removal was tested after incubating MIP and NIP films in water, for 15 minutes. The Rct values in the Nyquist increased and the peak currents in the CV data decreased, both in NIP (Figure 1C) and MIP films (Figure 1D). Considering the NIP alone, this behavior could be linked to the exit of conductive oligomeric structures of PANI from the polymeric network, something that could have happened also in the MIP film. As the MIP showed a more intense effect than the NIP, this could reflect the additional exit of HIS from the polymeric network. Overall, HIS is positively charged under the test conditions, thereby establishing ionic interactions with the negatively charged iron redox probe and contributing to improve the charge-transfer properties at the electrode surface

when it is there. Yet, the effect of the exit of HIS from the polymeric network is a balance between its non-conductive features and its ionic charge, and therefore its impact upon the Rct may vary.

Overall, these results confirmed an effective removal of HIS form the MIP films (when compared to the NIP) and the great stability of the PANI film when exposed to water.

3.5. Morphological characterization of the biosensor

Raman spectroscopy with a 785 nm laser gives valuable chemical information about gold materials and allows following-up their subsequent chemical modification. Raman spectra has been collected at different stages of the biosensor assembly Figure S3, specifically clean Au-SPE (Figure S3 A), after Cysteamine (Figure S3 B), MIP films (Figure S3 C) and MIP film after removal the template with ultrapure water (Figure S3 D).

Thus, when cysteamine was added to the clean gold surface, a several of new peaks appeared at 400 and 1400 cm^{-1}, as described in the literature [22], [23]. The next step was the electropolymerization of the MIP (C), which compared to the previous two steps has some changes and appears an intense peak at 575.5 cm^{-1}. After the removal (D), the Raman shift decreased significantly (560.82 cm^{-1}), which may reveal the successful removal of HIS.

3.6. Main analytical Features

The main analytical features of Au/Cys/MIP and Au/Cys/NIP electrodes were evaluated by incubating first a drop of HIS standard solution on the working electrode for 20 minutes to allow HIS binding, and by following after the EIS electrical features of a standard iron redox probe casted on the three-electrode system This was repeated for (i) increasing HIS concentrations to quantify the behavior of

these electrodes, over a wide concentration range, and for (ii) independent electrodes (using a minimum of 3).

The behavior of the Au/Cys/MIP electrodes is presented in Figure 3A, showing a typical Nyquist plot with blank solution and HIS concentrations ranging from 100 nM to 1 mM (left), prepared in lithium perchlorate, and the corresponding calibration curve, plotting absolute R_{ct} values against log concentration of HIS. The calibration plot evidences error bars that correspond to three independent sensors, with three independent calibrations, thereby confirming the excellent reproducibility of the analytical system. The linear trend was observed from 500 nM and 1mM, with an average slope of 1992.2 Ω/decade. The minimum squared correlation coefficient of all calibrations was 0.9957, and the average limit of detection was 210 nM. The corresponding Au/Cys/NIP evaluations are also shown (Figure 3B) and evidence a more random response against increasing HIS concentrations, thereby confirming the existence of non-specific binding of HIS to the PANI surface.

In general, increasing concentrations of HIS yielded increasing R_{ct} values with a linear behavior within a wide range of concentrations. This behavior revealed mostly the non-conductive properties of HIS, which were probably dominating the effect of the cationic charge of HIS. This was probably related to the higher concentrations of HIS reached at the surface in the calibration procedure, when compared to the template removal stage.

3.7. Selectivity test

Selectivity evaluations were made by means of a competitive assay against other biogenic amine that could be present in fish. TYR was considered herein, because it is a typical interfering species for HIS readings [2], [24]. This assay involved two independents sensing units and compared the effect of a single solution of 10 µM HIS and that of a mixed solution of 10 µM HIS and 10 µM TYR. It consisted

in collecting first the signal of the blank (lithium perchlorate) in both sensing units and after the signal generated by the incubation of the single solution of HIS (in one sensing unit) and the mixed solution of HIS and TYR (in another sensing unit).

Figure 4A shows the Nyquist plots of the Au/Cys/MIP electrodes evaluated under these conditions. The average percentage deviation upon the direct readings of HIS produced by TYR was +1.59 % (Figure 4B). Overall, these results confirmed that TYR had no interfering effect upon the HIS response and that the Au/Cys/MIP device was selective in the presence of other biogenic amine.

3.9 Samples Analysis

As proof-of-concept, Au/Cys/MIP devices were applied to the analysis of real samples. Two different fishes, sardine and mackerel, were used for this purpose. These samples were acquired in a supermarket, kept at room temperature and then frozen at three different timings (0 h; 12 h and 24 h), to allow the formation of biogenic amines [2]. As expected concentrations were unknown, two different dilution degrees (1000× and 100×) were used to check the biosensor response. These samples were also diluted in water, targeting the future direct analysis of samples, without any pre-treating procedures.

The typical results obtained are shown in Figure 5. In general, it was clear that the increasing time lead to an increasing amount of HIS in the samples, which was already expected due to the occurrence of fish degradation at ambient temperature. A total of 12h was enough to promote a significant increase of the HIS concentration in the sardine, while in the Mackerel samples a continuous increase was observed throughout time, being more significant for the 24h (Figure S4). Moreover, the lower dilution factor in both samples was always linked to higher R_{ct} values, thereby confirming their higher concentration in HIS.

The real concentration of HIS in these samples was found by the known addition method, as the samples were spiked with known and increasing amounts of HIS. These tests were made for samples exposed for 12 h to ambient temperature, as these were still below the typical linear response of the biosensors. Thus, the background (real) concentration in the samples was calculated by interacting with the standard addition method for a logarithm response in *x* axis [25]. The experimental data obtained is shown in Figure S5 and represents the spiked samples with known concentrations of HIS, using water as blank (t12) for each type of fish. Considering the reading of three independent sardine samples, the calculated concentration was 1.7×10^{-7} ($\pm4.4\times10^{-8}$) M. The corresponding procedure involving mackerel samples yielded average values of 3.5×10^{-7} ($\pm6.4\times10^{-8}$) M. In general, these results were in agreement with the direct sample readings, considering that the sardine samples had higher HIS concentrations, regardless the time of exposure to ambient temperature.

Overall, the results obtained demonstrated that the electrode was selective and able to detect HIS concentrations, even when the concentrations of HIS in the samples were below the linear response range of the biosensor. The biosensor device may be further employed to follow-up fish degradation and the formation of biogenic amines.

4. Conclusions

This work demonstrated the possibility of assembling an HIS biosensing device employding quick, expeditious and low-cost procedures. In these, the biorecognition element was produced *in-situ*, within few seconds, and the *on-site* detection of HIS in aquatic environment is also allowed, requiring only a 20 minutes incubation period.

In terms of analytical performance, the Au/Cys/MIP device displayed very good analytical features, demonstrating high sensitivity over a wide range of linear response, good selectivity against another competing biogenic amine, and ability to be applied to the analyses of real samples. The device may

be further employed to follow-up fish degradation and the formation of biogenic amines, which may be an interesting approach for food safety purposes.

Acknowledgements

The authors acknowledge national funding to the National Foundation for Science and Technology, I.P., and European funding to FEDER (European Funding or Regional Development), via COMPETE2020 – POCI (operational program for internationalization and competitiveness), through projects PTDC/MAR-BIO/6044/2014 and PTDC/AAG-TEC/5400/2014.

References

[1] A. Balan *et al.*, "Histamine detection using functionalized porphyrin as electrochemical mediator," *Comptes Rendus Chim.*, vol. 21, no. 3–4, pp. 270–276, 2017.

[2] P. Taylor and L. Prester, "Biogenic amines in fish , fish products and shellfish," *Food Addit. Contam.*, no. November, pp. 37–41, 2011.

[3] A. Veseli *et al.*, "Electrochemical determination of histamine in fish sauce using heterogeneous carbon electrodes modified with rhenium(IV) oxide," *Sensors Actuators, B Chem.*, vol. 228, pp. 774–781, 2016.

[4] M. M. G. Niraj and S. Pandey, "HISTAMINE BIOSENSOR: A REVIEW," *Int. J. Pharm. Sci. Res.*, vol. 3, no. 11, pp. 4158–4168, 2012.

[5] A. Geto, M. Tessema, and S. Admassie, "Determination of histamine in fish muscle at multi-walled carbon nanotubes coated conducting polymer modified glassy carbon electrode," *Synth. Met.*, vol. 191, pp. 135–140, 2014.

[6] S. K. Krishnan, E. Singh, P. Singh, M. Meyyappan, and H. S. Nalwa, "A review on graphene-based nanocomposites for electrochemical and fluorescent biosensors," *RSC Adv.*, vol. 9, no. 16, pp. 8778–8881, 2019.

[7] E. Bongaers *et al.*, "A MIP-based biomimetic sensor for the impedimetric detection of histamine in different pH environments," *Phys. Status Solidi Appl. Mater. Sci.*, vol. 207, no. 4, pp. 837–843, 2010.

[8] F. Barahona, B. Albero, J. L. Tadeo, and A. Martín-Esteban, "Molecularly imprinted polymer-hollow fiber microextraction of hydrophilic fluoroquinolone antibiotics in environmental waters and urine samples," *J. Chromatogr. A*, vol. 1587, pp. 42–49, 2019.

[9] M. Akhoundian, A. Rüter, and S. Shinde, "Ultratrace detection of histamine using a molecularly-imprinted polymer-based voltammetric sensor," *Sensors (Switzerland)*, pp. 1–10, 2017.

[10] K. M. A. El-Nour, E. T. A. Salam, H. M. Soliman, and A. S. Orabi, "Gold Nanoparticles as a Direct and Rapid Sensor for Sensitive Analytical Detection of Biogenic Amines," *Nanoscale Res. Lett.*, vol. 12, no. 1, 2017.

[11] A. R. Cardoso, A. P. M. Tavares, and M. G. F. Sales, "Sensors and Actuators B : Chemical In-situ generated molecularly imprinted material for chloramphenicol electrochemical sensing in waters down to the nanomolar level," *Sensors Actuators B. Chem.*, vol. 256, pp. 420–428, 2018.

[12] F. Horemans *et al.*, "Sensors and Actuators B : Chemical MIP-based sensor platforms for the detection of histamine in the nano- and micromolar range in aqueous media," *Sensors Actuators B. Chem.*, vol. 148, no. 2, pp. 392–398, 2010.

[13] A. Pietrzyk, S. Suriyanarayanan, W. Kutner, R. Chitta, and F. D. Souza, "Selective histamine piezoelectric chemosensor using a Recognition Film of the Molecularly Imprinted Polymer of Bis (bithiophene) Derivatives," *Analytical Chemistry*, vol. 81, no. 7, pp. 2633–2643, 2009.

[14] P. Tharmaraj, K. Pandian, K. Chitra, S. Devi, and S. Meenakshi, "Aniline-mediated synthesis of carboxymethyl cellulose protected silver nanoparticles modified electrode for the differential pulse anodic stripping voltammetry detection of mercury at trace level," *Ionics*

405 *(Kiel).*, 2019.
406 [15] E. Pashai, G. D. Najafpour, M. Jahanshahi, and M. Rahimnejad, “Highly Sensitive
407 Amperometric Sensor Based on Gold Nanoparticles Polyaniline Electrochemically Reduced
408 Graphene Oxide Nanocomposite for Detection of Nitric Oxide,” *Int. J. Eng.*, vol. 31, no. 2, pp.
409 188–195, 2018.
410 [16] A. Chen and B. Shah, “Electrochemical sensing and biosensing based on square wave
411 voltammetry,” *Anal. Methods*, vol. 5, no. 9, pp. 2158–2173, 2013.
412 [17] D. A. Armbruster and T. Pry, “Limit of Blank, Limit of Detection and Limit of Quantitation,”
413 vol. 29, pp. 49–52, 2008.
414 [18] F. T. C. Moreira, R. A. F. Dutra, J. P. C. Noronha, J. C. S. Fernandes, and M. G. F. Sales,
415 “Novel biosensing device for point-of-care applications with plastic antibodies grown on Au-
416 screen printed electrodes,” *Sensors Actuators, B Chem.*, vol. 182, pp. 733–740, 2013.
417 [19] C. Dhand, M. Das, M. Datta, and B. D. Malhotra, “Recent advances in polyaniline based
418 biosensors,” *Biosens. Bioelectron.*, vol. 26, pp. 2811–2821, 2011.
419 [20] M. F. Frasco, L. A. A. N. A. Truta, M. G. F. Sales, and F. T. C. Moreira, “Imprinting
420 technology in electrochemical biomimetic sensors,” *Sensors*, vol. 17, no. 3, 2017.
421 [21] M. Peeters, “Molecularly Imprinted Polymers (Mips) for Bioanalytical Sensors : Strategies
422 for Incorporation of Mips into Sensing Platforms,” *Austin J. Biosens. Bioelectron.*, vol. 1, no.
423 3, pp. 1–5, 2015.
424 [22] Q. Ma *et al.*, “Surface-enhanced Raman scattering substrate based on cysteamine-modified
425 gold nanoparticle aggregation for highly sensitive pentachlorophenol detection,” *RSC Adv.*,
426 vol. 6, no. 88, pp. 85285–85292, 2016.
427 [23] A. Abbas, L. Tian, R. Kattumenu, A. Halim, and S. Singamaneni, “Freezing the self-assembly
428 process of gold nanocrystals,” *Chem. Commun.*, vol. 48, no. 11, pp. 1677–1679, 2012.
429 [24] A. Onal, “Current analytical methods for the determination of biogenic amines in foods,”

Food Chem., vol. 103, pp. 1475–1486, 2007.

[25] F. M. Salama, K. A. Attia, R. A. Said, A. El-Olemy, and A. M. Abdel-Raoof, "Disposable gold nanoparticle functionalized and bare screen-printed electrodes for potentiometric determination of trazodone hydrochloride in pure form and pharmaceutical preparations," *RSC Adv.*, vol. 8, no. 21, pp. 11517–11527, 2018.

[26] L. T. Román, "Dual enzymatic biosensor for simultaneous amperometric determination of histamine and putrescine," *FOOD Chem.*, vol. 190, pp. 818–823, 2016.

[27] W. Henao-escobar, O. Domínguez-renedo, and M. J. Arcos-martínez, "A screen-printed disposable biosensor for selective determination of putrescine," *Microchim Acta*, pp. 687–693, 2013.

[28] M. A. Alonso-lomillo, O. Domínguez-renedo, P. Matos, and M. J. Arcos-martínez, "Disposable biosensors for determination of biogenic amines," *Anal. Chim. Acta*, vol. 665, pp. 26–31, 2010.

[29] S. Piermarini *et al.*, "Detection of Biogenic Amines in Human Saliva Using a Screen-Printed Biosensor," *Anal. Lett.*, vol. 2719, no. May, 2010.

[30] I. Apetrei and C. Apetrei, "Amperometric Biosensor Based on Diamine Oxidase/Platinum Nanoparticles/Graphene/Chitosan Modified Screen-Printed Carbon Electrode for Histamine Detection," *Sensors*, vol. 16, pp. 1–15, 2016.

[31] C. M. Keow, F. A. Bakar, A. B. Salleh, L. Y. Heng, and R. Wagiran, "Screen-printed Histamine Biosensors Fabricated from the Entrapment of Diamine Oxidase in a Photocured Poly (HEMA) Film," *Electrochem. Sci.*, vol. 7, pp. 4702–4715, 2012.

[32] S. Pérez, J. Bartrolí, and E. Fàbregas, "Amperometric biosensor for the determination of histamine in fish samples," *Food Chem.*, vol. 141, pp. 4066–4072, 2013.

[33] M. Bhargavi, N. Nesakumar, S. Sethuraman, U. Maheswari, J. Bosco, and B. Rayappan, "Development of electrochemical biosensor with ceria – PANI core – shell nano-interface for

the detection of histamine," *Sensors Actuators B. Chem.*, vol. 199, pp. 330–338, 2014.

[34] Y. R, F. N, T. M, T. S, S. O, and K. K, "Bioelectrochemical Determination at Histamine Dehydrogenase-based Electrodes," *Electrochemistry*, vol. 76, pp. 600–602, 2008.

[35] R. Kurita, K. Hayashi, T. Horiuchi, and O. Niwa, "Differential measurement with a microfluidic device for the highly selective continuous measurement of histamine released from rat basophilic leukemia cells (RBL-2H3)," *Lab Chip*, vol. 2, pp. 34–38, 2002.

[36] K. Yamamoto, K. Takagi, K. Kano, and T. Ikeda, "Bioelectrocatalytic Detection of Histamine Using Quinohemoprotein Amine Dehydrogenase and the Native Electron Acceptor Cytochrome c-550," *Electroanalysis*, vol. 13, pp. 375–379, 2001.

[37] M. Niculescu, C. Nistor, I. Fre, P. Pec, B. Mattiasson, and E. Cso, "Redox Hydrogel-Based Amperometric Bienzyme Electrodes for Fish Freshness Monitoring," *Anal. Chem.*, vol. 72, no. 7, pp. 1591–1597, 2000.

[38] W. Ye, Y. Xu, L. Zheng, Y. Zhang, M. Yang, and P. Sun, "A Nanoporous Alumina Membrane Based Electrochemical Biosensor for Histamine Determination with Biofunctionalized Magnetic Nanoparticles Concentration and Signal Amplification," *Sensors*, vol. 16, no. 1767, 2008.

[39] L. E. Delle *et al.*, "Impedimetric immunosensor for the detection of histamine based on reduced graphene oxide," *Phys. Status Solidi Appl. Mater. Sci.*, vol. 1334, no. 6, pp. 1327–1334, 2015.

[40] M. Yang, J. Zhang, and X. Chen, "Competitive electrochemical immunosensor for the detection of histamine based on horseradish peroxidase initiated deposition of insulating film," *J. Electroanal. Chem.*, vol. 736, pp. 88–92, 2015.

Legends for figures

Figure 1 Schematic illustration of electrochemical biosensor for detection of HIS (MIP and NIP): (A) Cleaning of Au/Cys; (B) Electro polymerization of MIP/NIP; (C) and (D) Template removal

Figure *1*

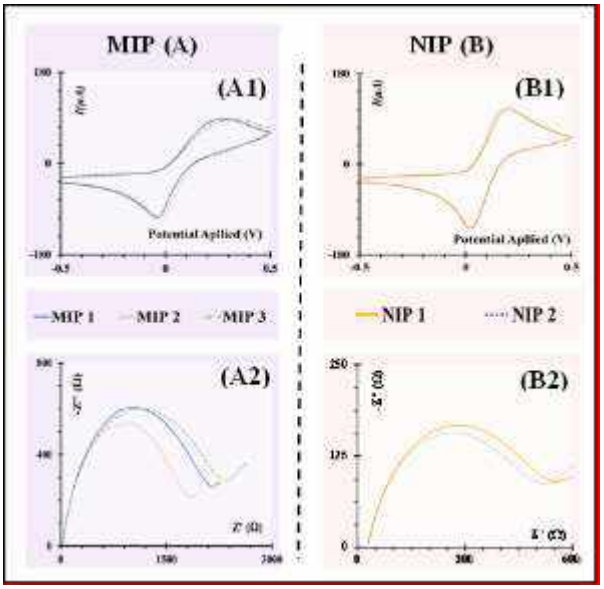

Figure *2* Reproducibility of electrochemical biosensor for detection of HIS: (A) Electro polymerization of MIP; (B) Electro polymerization of NIP; and comparison of different assays

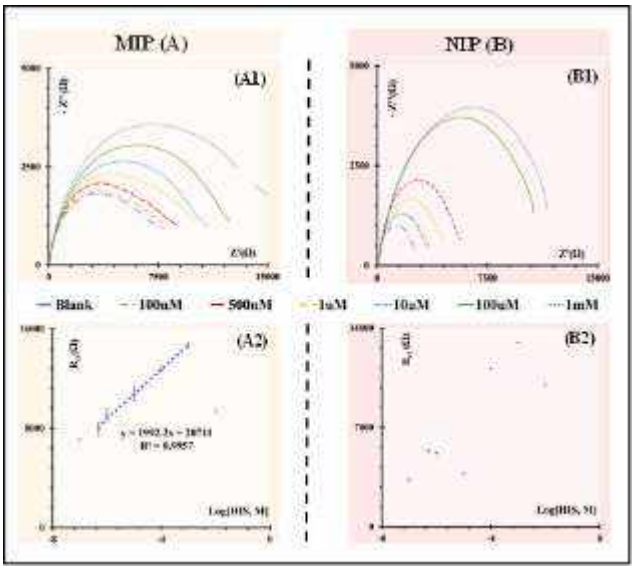

Figure 3 EIS Au/Cys/MIP (A1) and Au/Cys/NIP (B1) sensor, and the corresponding calibration curves (A2 and B2)

Figure 4 Selectivity behavior of the biosensor for HIS (1.00×10^{-5} M) against TYR (1.00×10^{-5} M)

Figure 5 EIS measurements in Au/Cys/MIP sensor after 20 minutes incubation, in standard solutions of HIS, prepared in diluted fish water in different times. t0 (A and B); t12 (C and D); t24 (E and F).

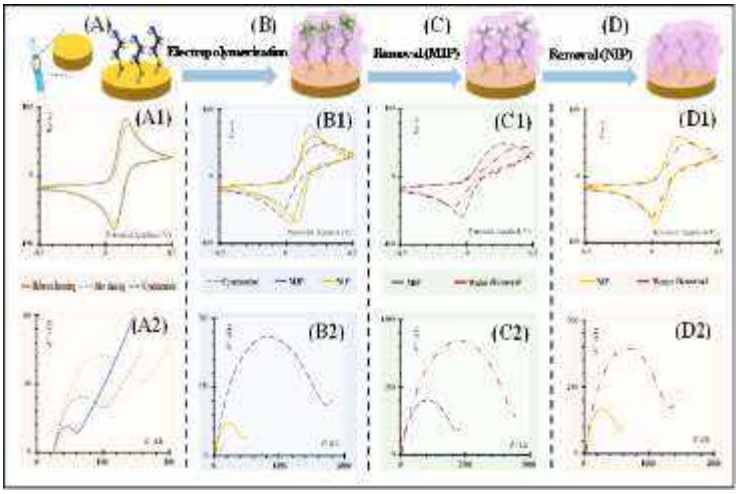

Figure 1

505 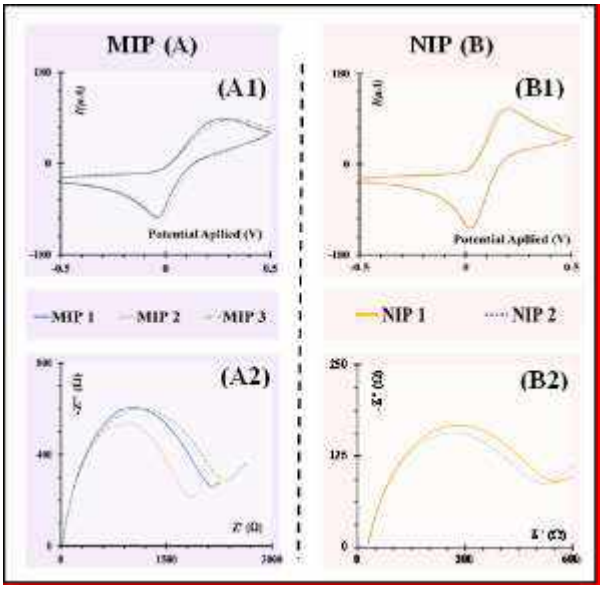

506

507 **Figure 2**

508

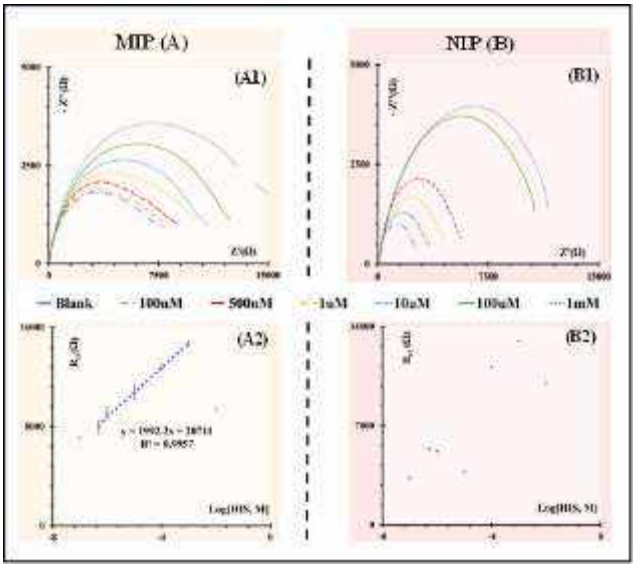

509

510 **Figure 3**

511

512 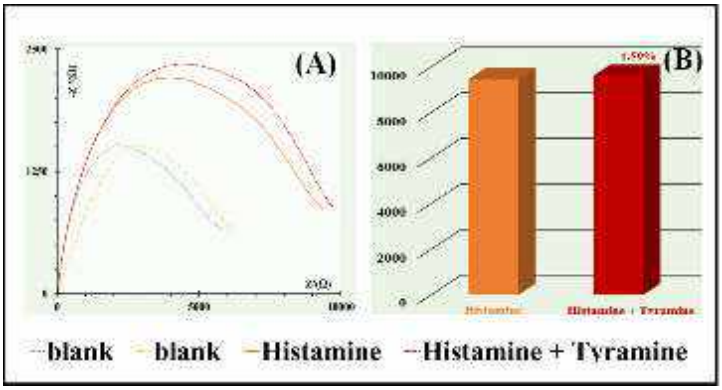

513 **Figure 4**

514

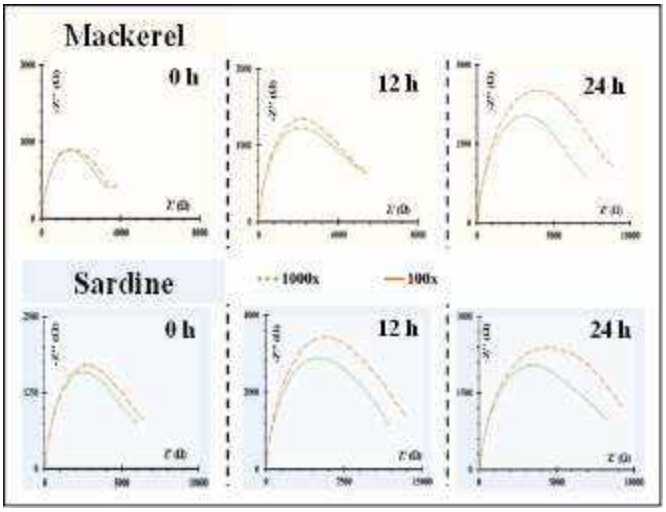

Figure 5

518 **Table 1-** Enzyme-based histamine electrochemical biosensors and the most relevant data about each work.

Support material	Enzyme	Brief Biosensing approach	Technical approach	LOD (µM)	Linear Range (µM)	Ref.
Carbon	**HISTdh**	TTF was screen-printed into a carbon ink to decrease the working potential in AMP. HISTdh enzyme was immobilized after on the TTF modified SPE of carbon by cross-linking with glutaraldehyde (GA) and bovine serum albumin (BSA).	CE AMP	4.6	—	[26]
Carbon	**PSAO**	Immobilization of PSAO using a Nafion solution. MWCNTs was used along with MnO_2 acting as mediator.	MWCNTs AMP	3.0	—	[27]
Carbon	**DAO** **HRP**	Covalent immobilization the enzymes using an aryldiazonium salt, hydroxysuccinimide and carbodiimide. Ferrocene acted as mediator.	CE AMP	0.4	—	[28]
Carbon	**DAO**	The enzyme is entrapped by crosslinking with GA and BSA, and Prussian blue acts as mediator for AMP reading.	CE AMP	10	—	[29]
Carbon	**DAO**	DAO was immobilized on a nanostructured composite matrix of platinum NPs, graphene and chitosan, present on an SPE of carbon, for a direct detection of H_2O_2.	CE CV	0.025	0.1 to 300	[30]
Carbon	**DAO**	SPE with a carbon paste working electrode, modified to entrap DAO in a poly(2-hydroxyethyl methacrylate), prepared via photocuring process. The mediator was hexacyanoferrate (III).	CE AMP	18000	Up to 1690000	[31]
Carbon	**DAO** **HRP**	DAO and HRP are co-immobilized into a polysulfone/carbon nanotubes/ferrocene membrane by means of phase inversion technique onto screen-printed electrodes.	CNTs AMP	0.17	0.3 to 20	[32]
Carbon	**DAO**	A GCE was modified with CeO_2/PANI composite for sensing histamine using DAO. CeO_2/PANI core–shell NPs were prepared by hydrothermal method.	GCE CV AMP	49	450 1100	[33]
Carbon	**HISTdh**	HISTdh was co-immobilized with a poly(1-vinylimidazole), which was complexed with [Os(2,2'-dipyridylamine)2Cl] (osmium acts as mediator), and a cross-linker, poly(ethylene glycol) diglycidyl ether, directly on a GCE.	GCE AMP	2	2 to 30	[34]
Carbon	**HRP** **HISTdh**	Differential analysis in a micro-fluidic device of two electrodes containing Os-polyvinylpyridine based mediator with horseradish peroxidase (Os-gel-HRP); in these, only one electrode contained HISTox, thereby promoting a differential signal.	GCE AMP	0.025	0.5 to 500	[35]
Gold	**QH-AmDH**	Au electrodes modified with Bis(4-pyridyl)disulphide and having QH-AmDH and Cyt c-550 co-entrapped at the electrode surface. Cyt c-550 is a native electron acceptor and acts as mediator.	AuE CV	0.5	—	[36]
Graphite	**HRP** **HISTox**	A flow injection three-electrode system with wall-jet type was used to co-immobilize amine oxidase (AO) and HRP, by adsorption onto graphite electrodes and	Graphite electrode	0.33	1.0 to 100	[37]

		crosslinking to an Os-based redox polymer, acting as mediator	AMP			

AMP – Amperometry; AuE – gold electrodes; ; CE – carbon electrode; Cyt c-550 – cytochrome c-550; CV – Cyclic voltammetry; DAO – diamine oxidase; HMD - histamine deshydrogenase; HISTdh –histamine dehydrogenase; HISTox – histamine oxidase; HRP – horseradish peroxidase; LOD – Limit of detection; MAO – monoamine oxidase; MWCNTs – multiwall carbon nanotubes; NPs – nanoparticles; PtE – platinum electrode; PSAO – pea seedling amino oxidase; ; PUO - putrescine oxidase; QH-AmDH – Quinohemoprotein Amine Dehydrogenase; SPEs - Screen-printed electrodes;TAO – tyramine oxidase; TTF – Tetrathiafluvalene.

Table 2- Antibody-based histamine electrochemical biosensors and the most relevant data about each work.

Support material	Brief Biosensing approach	Technical approach	LOD (µM)	Linear Range (µM)	Ref.
Alumina	Magnetic NPs conjugated with His antibody were incubated in the sample for pre-concentration. These conjugates were captured later in an alumina nanoporous membrane also containing His antibody. Capturing the NPs resulted in a blocking effect monitored by EIS.	Magnetic NPs EIS	0.003	1.0 to 4000	[38]
GO	Graphene oxide on glass was modified with a His antibody to detect the presence of an His BSA conjugate.	EIS SPR	0.1	0.1 to 1.0	[39]
Graphene	His antibody was attached to a graphene surface. Then, the free histamine (from the sample) and HRP tagged histamine molecules competed to bind to the antibodies. HRP further catalyses the polymerization of 3,3-dimethoxybenzidine (PDB) in the presence of H_2O_2 to produce the deposition of an insulating PDB film, resulting in the decrease of the electrochemical current. The more insulating, the less free histamine present in the sample. The redox mediator was ferricyanide.	SWV	0.055	0.11 to 110	[40]

GO – graphene oxide; His – Histamine; HRP - horseradish peroxidase (HRP); NPs – nanoparticles; PDMS – polydimethylsiloxane; PBD – 3,3-dimethoxybenzidine; SWV – square-wave voltammetry; SPR - Surface Plasmon Resonance.

Supplementary Material

to

In-situ production of Histamine-imprinted polymeric materials for electrochemical monitoring of fish

Verónica M. Serrano, Ana R. Cardoso, Mário Diniz, M. Goreti F. Sales*

BioMark/CEB, ISEP, R. Dr. António Bernardino de Almeida, 431, 4200-072 Porto, Portugal

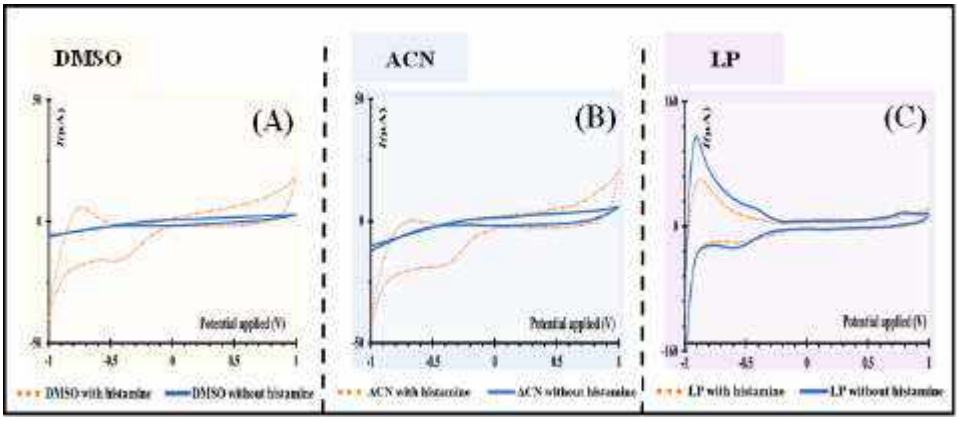

Figure S1. Results obtained using different chemical compounds for the determination of the best electrolyte for these assays.

559 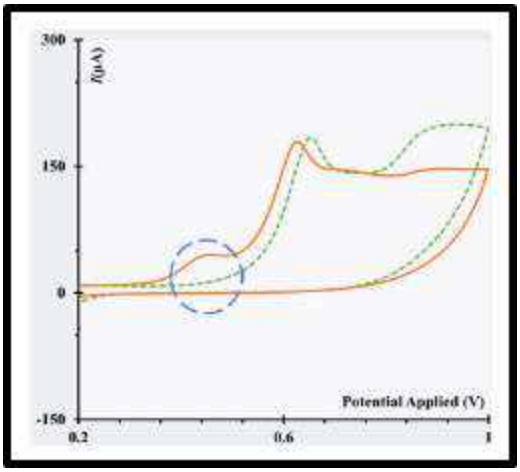

560 **Figure S2.** Cyclic voltammograms of a solution of Aniline (orange, regular line) prepared in lithium
561 perchlorate and a solution of HIS (green, dotted line) also prepared in lithium perchlorate to find the
562 potential peak.

563

564

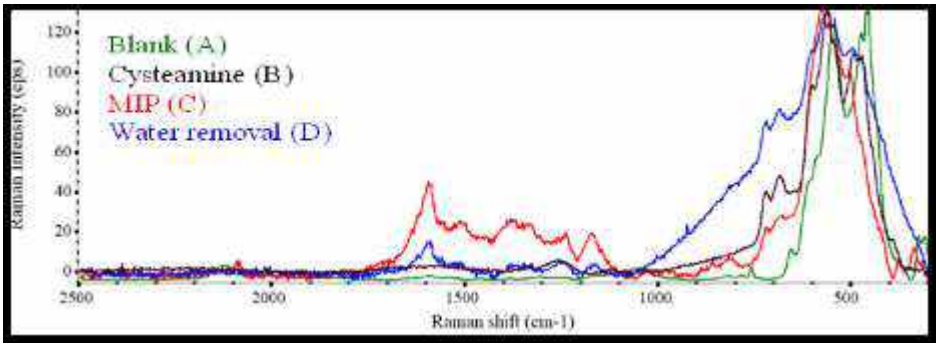

565

Figure S3- Raman spectra of several materials for G-SPE. Blank (A) corresponds to G-SPE without any treatment; Au/Cys (B); Electropolymerization of MIP (C) and removal template with ultrapure water (D).

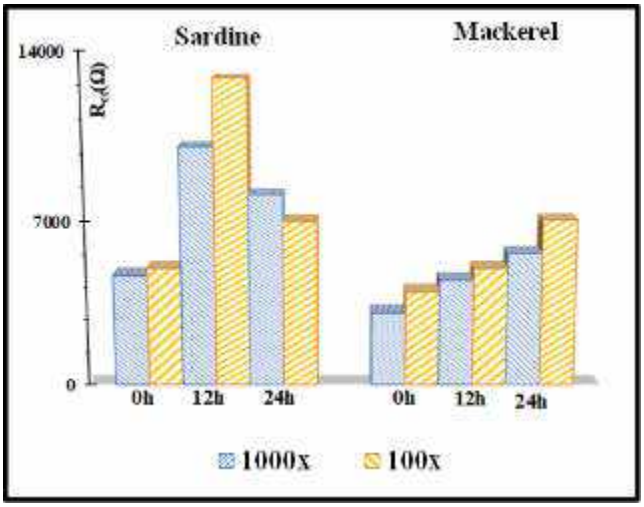

Figure S4. R_{ct} values to follow the real concentration of HIS in different times and dilutions. The solutions were prepared in LP.

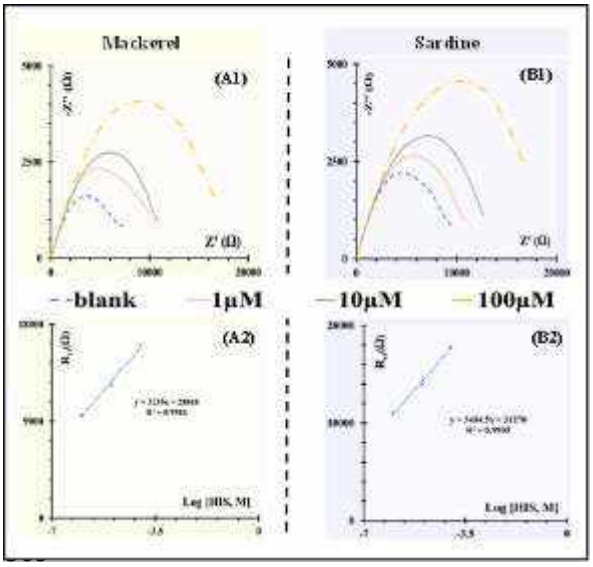

Figure S5. EIS (1, top) measurement in MIP sensor, and the corresponding calibration curves (2, bottom), in 5.0×10^{-3} M $[Fe(CN)_6]^{3-}$ and 5.0×10^{-3}M $[Fe(CN)_6]^{4-}$, in standard solutions of HIS of increasing concentrations, of Mackerel (A) and Sardine (B) samples, prepared in diluted blank fish water medium.